Journal of Inorganic Biochemistry 105 (2011) 1767–1773

Contents lists available at SciVerse ScienceDirect

Journal of Inorganic Biochemistry

journal homepage: www.elsevier.com/locate/jinorgbio

A series of mononuclear Co(III) complexes using tridentate *N,O*-donor ligands: Chemical properties and cytotoxicity activity

Elizabeth Teixeira Souza [a], Paulo José Sousa Maia [a], Érica Melo Azevedo [a], Carlos Roland Kaiser [a], Jackson Antônio Lamounier Camargos Resende [b], Carlos Basílio Pinheiro [c], Tassiele Andrea Heinrich [d], Roberto Santana da Silva [d], Marciela Scarpellini [a,*]

[a] *Instituto de Química, Universidade Federal do Rio de Janeiro, 21945–970, Rio de Janeiro, RJ, Brazil*
[b] *Departamento de Química Inorgânica, Instituto de Química, Universidade Federal Fluminense, 24020–150, Niterói, RJ, Brazil*
[c] *Departamento de Física, Instituto de Ciências Exatas, Universidade Federal de Minas Gerais, 31270–901, Belo Horizonte, MG, Brazil*
[d] *Departamento de Física e Química, Faculdade de Ciências Farmacêuticas de Ribeirão Preto, Universidade de São Paulo, 14040–903, Ribeirão Preto, SP, Brasil*

ARTICLE INFO

Article history:
Received 22 June 2011
Received in revised form 8 September 2011
Accepted 8 September 2011
Available online 16 September 2011

Keywords:
Cobalt complexes
Hypoxia
Melanoma
Prodrugs
B16F10

ABSTRACT

Continuing our interest in tridentate ligands to develop new prototypes of cobalt-based metallodrugs for combating cancer, modifications in the backbone of **HL1**, [(2-hydroxybenzyl)(2-(pyridil-2-yl)ethyl]amine) were proposed in order to modulate the redox potential of new Co(III) complexes. Three ligands with electron withdrawing groups were synthesized: **HL2**: [(2-hydroxy-5-nitrobenzyl)(2-(pyridil-2-yl)ethyl] amine); **HL3**: [(2-hydroxybenzyl)(2-(pyridil-2-yl)ethyl]imine) and **HL4**: [(2-hydroxy-5-nitrobenzyl)(2-(pyridil-2-yl)ethyl]imine). They were used to obtain the respective mononuclear complexes **2**, **3** and **4**, which are discussed compared to the previous reported complex **1** (obtained from **HL1**). The new complexes were characterized and studied by several techniques including X-ray crystallography, elemental and conductimetric analysis, IR, UV–vis and ^{1}H NMR spectroscopies, and electrochemistry. The substitutions of the group in the *para* position of the phenol (**HL1** and **HL2**) and the imine instead of the amine (**HL3** and **HL4**), promote anodic shifts in the complexes reduction potentials. The influence of these substitutions in the biological activities of the Co(III) complexes against the murine melanoma cell line (*B16F10*) was also evaluated. Little effect was observed on cellular viability decrease for all free ligands, however the coordination to Co(III) enhances their activities in the following range: **1**>**4**≈**2**>**3**. The data suggest that no straight correlation can be addressed between the reduction potential of the Co(III) center and the cell viability.

1. Introduction

The development of a solid tumor leads to three distinctive areas based on the availability of O_2 in consequence of the different rates of angiogenesis and cellular proliferation. A common feature that solid tumors share is an oxygenated shell (2 – 9% of O_2), an intermediary hypoxia area (≤2% of O_2) and an anoxia core (≤ 0.02% of O_2) [1]. The hypoxia area is well known to be resistant to the two most worldwide employed cancer therapies: the radio and the chemotherapies. This fact depends on the O_2 levels necessary for the generation of radicals, and on the amount of drug that reaches the area through the blood vessels. Besides this resistance, in the last two decades, it has been demonstrated that hypoxia has a wider role in the tumor and is also related to the increase of some factors such as metastasis, selection of more malignant phenotype, angiogenesis, mutation rates, resistance to apoptosis, decrease of DNA repair and mutagenesis [1–3]. As a consequence of the different O_2 environments in the tumor, combating cancer has been a tough challenge. As a unique feature of solid tumors, hypoxia represents a good target for the development of site selective anticancer prodrugs. Most of the molecules designed under the concept of prodrugs activated by hypoxia are organic compounds and some of them are already in clinical trials [2]. However, coordination compounds have also been exploited as bioreductible agents, mainly those containing Pt(IV), Ru(III) and Co(III) centers [4–25]. Interested in cobalt-based prodrugs, we have exploited the use of tridentate *N,O*-donor ligands to obtain Co(III) complexes and to evaluate their biological activities [25]. As previously reported [26], the use of the ligand **HL1**, 2-((2-(pyridin-2-yl)ethylamino)methyl)phenol (Fig. 1), resulted in a mononuclear complex (complex **1**) that is able to inhibit the colony growing and the cellular death of *Saccharomyces cerevisiae* harvested in fermentative metabolism. This growth medium is anaerobic and resembles the hypoxia tumor cells, which encouraged us to investigate the activity of these complexes against cancer cells. Here, in addition to the activity of complex **1** against the murine melanoma cell line *B16F10*, the synthesis, characterization and cytotoxic activity results of three other complexes (**2** – **4**) are presented. These complexes were designed with

* Corresponding author. Tel.: +55 21 2562 7742; fax: +55 21 2562 7559.
E-mail address: marciela@iq.ufrj.br (M. Scarpellini).

0162-0134/$ – see front matter © 2011 Elsevier Inc. All rights reserved.
doi:10.1016/j.jinorgbio.2011.09.011

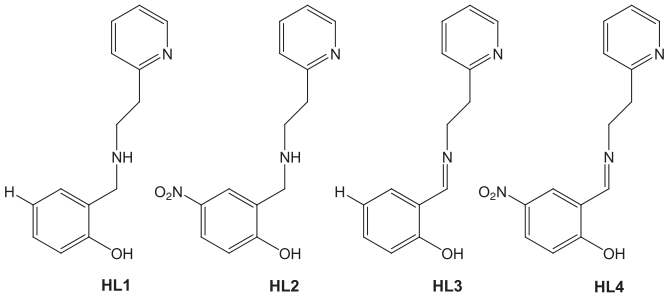

Fig. 1. Schematic views of ligands (**HL1 – HL4**).

ligands containing electron-withdrawing features (**HL2 – HL4**, Fig. 1) to modulate the reduction potential of the metal center in order to evaluate how it correlates with their antitumoral activities.

2. Experimental section

2.1. General remarks

Ligands **HL1** and **HL2** were prepared by the method previously described for **HL1**, which consists of the reduction of the respective imines **HL3** and **HL4** with $NaBH_4$ in methanol [27,28]. Complex **1** was synthesized and purified as previously described [26]. The ligand samples used in complexation syntheses and biological assays were purified by recrystallization. All of the chemicals for syntheses and analyses were of analytical grade and used without further purification. Elemental analyses were obtained in a Perkin-Elmer 2400 analyzer coupled to an AD-4 Perkin-Elmer balance. Infrared spectra of ligands and complexes were obtained from KBr pellets using a NICOLET MGNA FTIR-760 spectrophotometer. Electronic absorption spectra were recorded using a Cary-50 UV-visible spectrophotometer in methanol. Cyclic voltammograms were performed with a BAS Epsilon potentiostat, at room temperature (25 ± 1)°C, in methanol solutions, under argon atmosphere. A standard three-electrode cell was employed, where the electrode set was: a glassy carbon working, a platinum auxiliary and a Ag/AgCl pseudo-reference. $TBAPF_6$ [0.1 M] was used as supporting electrolyte and the ferrocenium-ferrocene couple [29] was employed to monitor the reference electrode potential ($E_{1/2} = 250$ mV vs Ag/AgCl, $\Delta E_p = 102$ mV for complex **2,** $E_{1/2} = 290$ mV vs Ag/AgCl, $\Delta E_p = 90$ mV for complex **3**, and $E_{1/2} = 349$ mV vs Ag/AgCl, $\Delta E_p = 95$ mV for complex **4**). ^{1}H (500 MHz) and ^{13}C NMR (125 MHz) spectra were recorded on a Bruker Avance-500 spectrometer, equipped with a 1.7 mm z-gradient probe head, and in DMSO-d_6 solutions referenced to TMS (tetramethylsilane). When necessary, experiments of 2D NMR (COSY, HSQC and HMBC) and DEPT-135 were also employed (data not shown).

2.2. Complexes syntheses

Complexes **2** – **4** were obtained by the same general procedure consisting of the slow addition of $Co(ClO_4)_2.6H_2O$ (1 mmol in 20 mL of methanol) to a methanol solution of the ligands **HL2 – HL4** (2 mmol in 20 mL). The reaction mixtures were gently heated under stirring for ca. 30 min, filtered off and left undisturbed to obtain the respective complexes as amorphous precipitates, which were further recrystallized.

$[Co(L2)_2]ClO_4 \bullet 1/3C_2H_5OH$, **2**. Recrystallization of complex **2** in methanol:acetonitrile (3:1) yielded red brown single crystals suitable for X-ray analysis and were also used for the other analyses. Yield: 144 mg, 38%. Decomposition point: 233 °C. FTIR (KBr, cm^{-1}): $\nu(NH_{sec})$, 3199; $\nu(CH_{Ar}/CH_{Alif})$, 3103–2975; $\nu(C=N/C=C)$, 1599–1492; $\nu(N=O)$, 1337; ν(C-O) 1294; ν(Cl-O), 1117–1085 and $\delta(CH_{Ar})$, 756. Elemental analysis: calc. for $C_{28}H_{28}ClCoN_6O_{10} \bullet 1/3C_2H_5OH$ (FW:

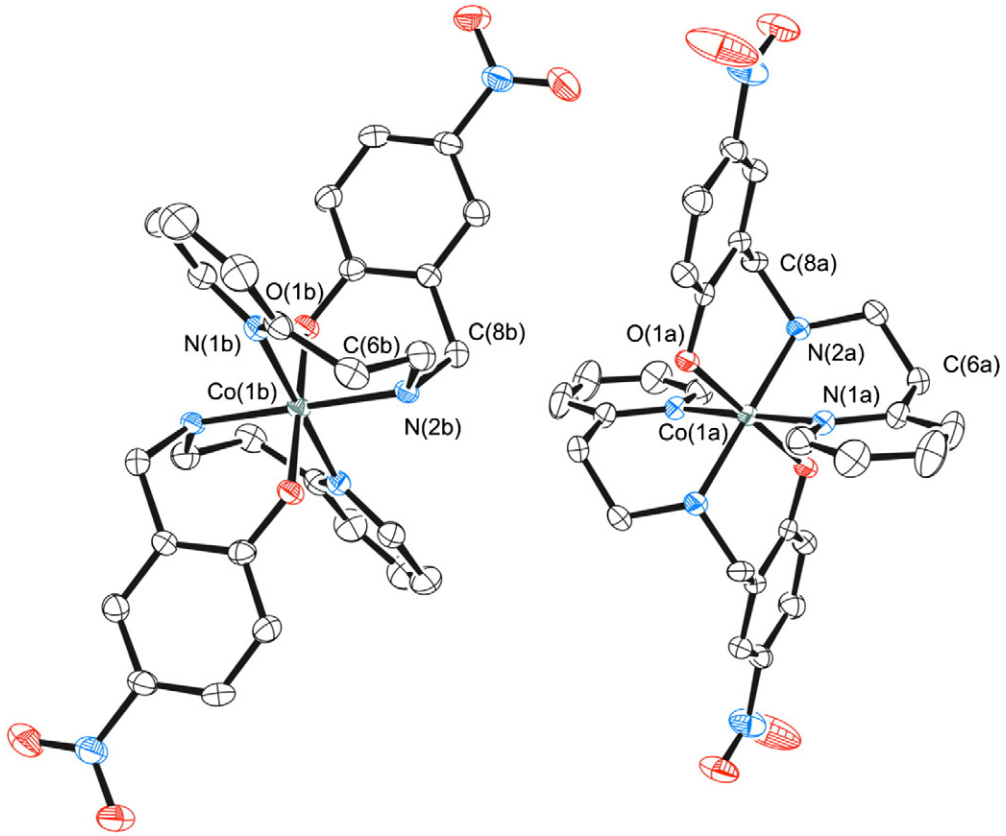

Fig. 2. Cartoons of the molecules **2a** and **2b** in the asymmetric unit of complex **2**, showing the atoms labeling and the 30% probability ellipsoids.

718.30 g mol^{-1}) calc. (found): C, 47.84 (47.93); H, 4.01 (4.21); N, 11.96 (11.70)%. $\Lambda_M = 138\ \Omega^{-1}\ mol^{-1}\ cm^2$ (electrolyte 1:1 in methanol) [30]. ^{1}H NMR (DMSO-d_6, 500 MHz, d = doublet, m = multiplet, t = triplet, bd = broad doublet, bt = broad triplet): δ 9.07 (d, J = 5.2), 8.06 (d, J = 2.6), 8.00-7.90 (m), 7.76-7.71 (m), 7.70-7.64 (m), 7.54 (d, J = 7.8), 7.42 (d, J = 7.3), 7.18 (t, J = 6.2), 6.92 (d, J = 8.8), 6.76 (d, J = 9.3), 4.57 (bd, J = 13.5), 3.97 (bt, J = 14.5), 3.89 (bt, J = 15.0), 3.43-3.32 (m), 3.12 (bd, J = 15.0), 2.99-2.91 (m), 2.71 (d, J = 11.5), 2.13-2.00 (m).

$[Co(L3)_2]ClO_4$•½CH_3OH, **3**. Brown single crystals of complex **3** suitable for X-ray analysis were obtained by recrystallization of the precipitate in pure ethanol. Yield: 285 mg, 40%. Decomposition point: 260 °C. FTIR (KBr, cm^{-1}): ν(C-H_{Ar}/C-H_{Alf}), 3589 – 3422; ν(C = N/C = C_{Ar}), 1623/1550-1450; ν(C-O) 1280; ν(Cl-O), 1109 and δ(CH_{Ar}), 765. Elemental analysis: calc. for $C_{28}H_{26}ClCoN_4O_6$•½CH_3OH (FW: 624.94 g mol^{-1}) calc. (found): C, 54.77 (55.23); H, 4.52 (4.30); N, 8.97 (9.20)%. $\Lambda_M = 137.6\ \Omega^{-1}\ mol^{-1}\ cm^2$ (electrolyte 1:1 in acetonitrile) [30]. ^{1}H NMR (DMSO-d_6, 500 MHz, bs = broad singlet, d = doublet, t = triplet, m = multiplet): δ 8.23 (1H, bs), 7.96 (1H, d, J = 5.8), 7.89 (1H, t, J = 7.7), 7.46 (1H, d, J = 7.4), 7.30-7.24 (2H, m), 6.97 (1H, t, J = 7.0), 6.59 (1H, d, J = 8.2), 6.48 (1H, t, J = 6.7), 4.45 (1H, bs), 4.20 (1H, bs), 3.71 (1H, bs), 2.60 (1H, bs). ^{13}C NMR (DMSO-d_6, 125 MHz): δ 168.8 (CH), 164.4 (C), 162.9 (C), 155.41 (CH), 140.8 (CH), 135.0 (CH), 134.2 (CH), 126.5 (CH), 124.4 (CH), 121.2 (CH), 120.1 (C), 115.8 (CH), 53.8 (CH_2), 34.5 (CH_2).

$[Co(L4)_2]ClO_4$•5H_2O, **4**. Single crystals of complex **4** were obtained by recrystallization in pure acetone which yielded dark red single crystals suitable for X-ray analysis. Yield: 236 mg, 30%. Decomposition point: 268 °C. FTIR (KBr, cm^{-1}): ν(C-H_{Ar}/C-H_{Alf}), 3078–2861; ν(C = N/C = C_{Ar}), 1633/1556-1449; ν(N = O), 1312; ν(C-O) 1248; ν(Cl-O), 1110 and δ(CH_{Ar}), 756. Elemental analysis: calc. for $C_{28}H_{24}ClCoN_6O_{10}$•5$H_2O$ (FW: 807.03 g mol^{-1}) calc. (found): C, 42.60 (42.62); H, 4.27 (4.34); N, 10.57 (10.65)%. $\Lambda_M = 88.1\ \Omega^{-1}\ mol^{-1}\ cm^2$ (electrolyte 1:1 in methanol) [29]. ^{1}H NMR (DMSO-d_6, 500 MHz, bs = broad singlet, m = multiplet, d = doublet, t = triplet) Fig. S1): δ 8.60 (1H, bs), 8.51 (1H, bs), 8.09-8.00 (2H, m), 7.80 (1H, d, J = 9.1), 7.57 (1H, d, J = 8.1), 7.40 (1H, t, J = 7.0), 6.60 (1H, d, J = 9.1), 4.49 (1H, bs), 4.21 (1H, bs), 3.47 (1H, bs), 2.17 (1H, bs). ^{13}C NMR (DMSO-d_6, 125 MHz): δ 171.9 (CH), 170.6 (C), 165.0 (C), 157.1 (CH), 143.1 (CH), 138.3 (C), 133.2 (CH), 130.8 (CH), 128.9 (CH), 126.7 (CH), 123.5 (CH), 121.8 (C), 55.0 (CH_2), 35.6 (CH_2).

2.3. In vitro cytotoxicity assays

Biological properties were assessed for ligands (**HL1 – HL4**) and complexes (**1** – **4**) which were assayed against the tumor cell line *B16F10* (murine melanoma). The cell line was cultured using the Roswell Park Memorial Institute (RPMI) adjusted to contain 1.5 g L^{-1} sodium bicarbonate, 4.5 g L^{-1} glucose at pH 7.0. All cells were kept in a humidified atmosphere with 5% CO_2 at 37 °C, supplemented with 10% fetal bovine serum and 1% of antibiotic/antimycotic. After reaching confluence, the cells were removed from the flasks using trypsin/EDTA (1×) and counted for the experiments. To evaluate the cytotoxic activity of compounds, cellular viability was determined by the MTT test [3-(4,5-dimethylthiazol-2-yl)-2,5-diphenyltetrazolim bromide], a colorimetric assay determined by the mitochondrial-dependent reduction of the soluble yellow tetrazolium salt to blue formazan crystals [31]. The cells were seeded into a 96-well plate (1.5×10^4 cells per well) in 200 μL of the appropriate complete medium 24 h prior to the beginning of the experiment. The stock solutions of the compounds were prepared in sterile DMSO and directly diluted into the medium in order to achieve different final concentrations, with a final concentration of maximum 2% DMSO (vehicle). Forty-eight hours after the addition of the complex or the vehicle, MTT (0.5 g L^{-1}) was added and the cells were incubated for a period of 3 h. The optical density was measured after dissolving the blue formazan crystals into 200 μL of DMSO, and the cell viability was determined by absorbance measurements at 570 nm. The amounts of surviving cells, compared to those of the untreated controls were determined.

2.4. X-ray crystal structure determination

Suitable single crystals for X-ray diffraction of complexes **2**, **3** and **4** were obtained by slow evaporation of methanol:acetonitrile (3:1), ethanol and acetone solutions, respectively. A remarkable characteristic of complex **4** is the expressive solvent lost when crystalline sample is removed from the crystallization solution. In order to keep the crystals stable during the X-ray diffraction experiment the sample of complex **4** had to be fast frozen. The procedure systematically twinned the samples, thus both X-ray diffraction measurements and, consequently, the structural refinements are limited by the poor crystalline sample quality.

Single crystals X-ray diffraction data of **2** and **3** were collected using a *Bruker Kappa CCD* equipped graphite-monochromatized MoKα radiation (0.71073 Å) at room temperature. The unit cell parameters were determined and refined using all reflections [32] and the data integration and scaling were realized with *EVALLCCD* program [33]. Absorption corrections were performed by multi-scan method implemented in *SADABS* program [34]. X-ray diffraction data collection for complex **4** was performed on an *Oxford-Diffraction GEMINI* diffractometer using graphite-Enhance Source MoKα radiation (λ = 0.7107 Å) at 130 K. Data integration and scaling of the reflections were performed with the *Crysalis suite* [35]. Final unit cell parameters were based on the fitting of all reflections positions. Analytical absorption corrections of the diffracted intensities were performed using *Crysalis suite* [36]. Program *XPREP* [37] was used for all data reduction.

The structures of all complexes were solved by direct methods using the *SHELXS* [37] program. For each compound, the positions of all atoms could be unambiguously assigned on consecutive difference Fourier maps. Solvent and counter ions molecules were observed in the structure of all compounds. Refinements were performed using *SHELXL* [37] based on F^2 through full-matrix least square routine. All but hydrogen atoms and perchlorate counter ion in complex **4** were refined with anisotropic atomic displacement parameters. The hydrogen atoms in the compounds were added in the structure in idealized positions and further refined according to the riding model [38]. Complexes **2**, **3** and **4** cartoons are represented in Figs. 2, 3 and 4, respectively. Solvents and counter ions were omitted for the sake of clarity. The unit cell of complex **2** is composed of two molecules of $[Co(L2)_2]$•ClO_4 with slight differences between them. In complex **3**, the perchlorate counter ion is disordered over two positions. In complex **4**, two acetone solvent molecules and a disordered perchlorate counter ion were observed in a large structural cavity (Fig. S2). The abnormal high peaks close to the Co atom, high R-values and goodness of fit parameters evidence complex **4** refinement problems. The crystallographic data for complexes **2** – **4** are given in Table 1, and the relevant structural parameters are listed in Table 2.

3. Results and discussion

3.1. Syntheses and characterization

All ligands were synthesized by direct condensation of the appropriate *para*-substituted salicylaldehyde with 2-2(aminoethylpyridine) according to previously reported methodologies [27,28]. Infrared and ^{1}H NMR spectroscopies, melting points and elemental analysis were used to confirm the purity of the ligands. Complexes **2** – **4** were prepared by the same methodology employed for complex **1**, and were isolated as single crystals by recrystallization in appropriate solvents. In order to guarantee the purity of the samples, only single crystals were used in the analyses of all complexes. Initially, the

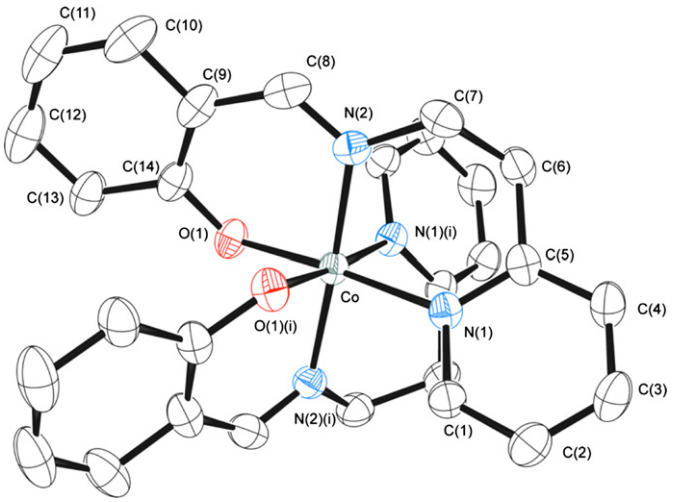

Fig. 3. Cartoons of complex **3**, showing the atoms labeling and the 30% probability ellipsoids.

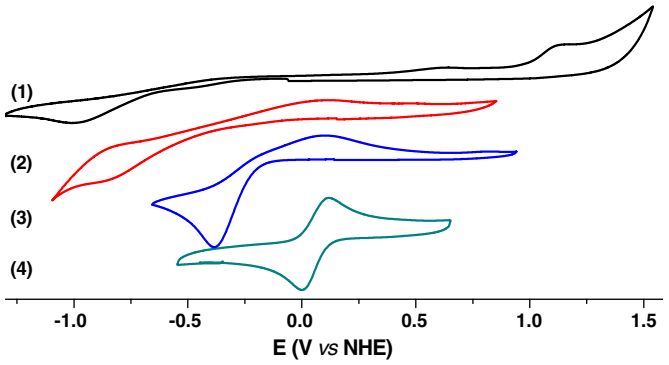

Fig. 5. Cyclic Voltammograms of **1**–**4** in methanol ($C = 1 \times 10^{-3}$ M, at 25 ± 1 °C, 0.1 M of $TBAPF_6$ as supporting electrolyte, glassy carbon working electrode, platinum wire auxiliary electrode, Ag/AgCl reference eletrode) at scan rates 100 $mV.s^{-1}$.

complexation reactions were checked out by infrared spectroscopy, where the main vibrations related to the ligand backbones were identified, in addition to the presence of bands around 1100 cm^{-1} assigned to the Cl-O perchlorate stretching [39]. Elemental analyses agree with mononuclear complexes in a ligand:metal ratio of 2:1, as observed for complex **1**, and confirmed by X-ray analysis. In solution, complexes **2** – **4** were studied in methanol in order to compare with the data reported for complex **1** [26]. Conductimetric analyses of all complexes are in the range for electrolytes of the type 1:1 [30], suggesting that the ligand:metal ratio (2:1) is maintained is solution.

3.2. Crystal structures

X-ray crystallographic data of all complexes revealed mononuclear cation complexes neutralized by one perchlorate anion. In all of the cases, the metal center Co(III) coordinates to two tridentate N_2O-donor ligand molecules, in distorted octahedral geometries. As observed for complex **1** [26], complex **2** also presents two crystallographically independent molecules (**2a** and **2b**) in the asymmetric unit (Fig. 2) which differ only in some angles and bond distances, as shown in Table 1. As also observed for complex **1**, the L_2^- ligand coordinates in a facial mode in both molecules (**2a** and **2b**). Then, atoms of the same nature are coordinate *trans* to each other in a such way one can consider the four nitrogen atoms occupying the equatorial plane [Co1A-N1A: 1.995 (4) Å and Co1A-N2A: 1.981 (13) Å], and the oxygen atoms lying in the axial plane [Co1A-O1A: 1.885 (3) Å]. A comparison of the coordination sphere of the Co(III) atom in complexes **1** [26] and **2** reveal that all bond lengths are shorter in complex **2**. As expected, the Co-O_{phenol} distance is the shortest one varying from 1.9107 (13) Å in complex **1** to 1.885 (3) Å in complex **2**, which reflects the electron withdrawing effect of the -NO_2 group.

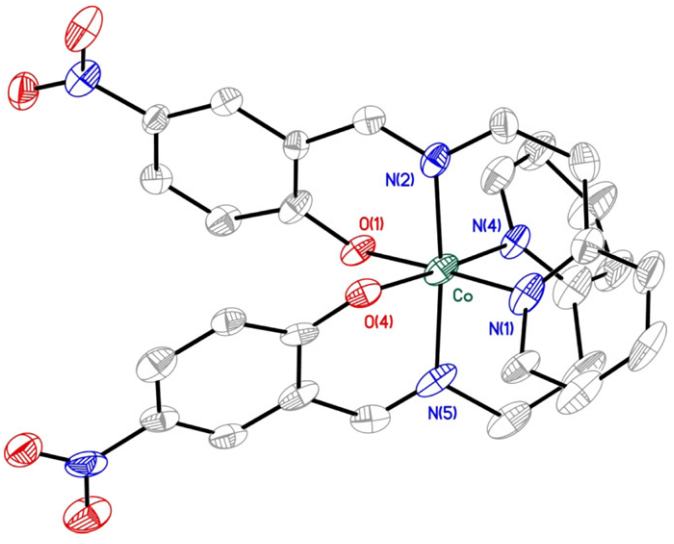

Fig. 4. Cartoons of complex **4**, showing the atoms labeling and the 30% probability ellipsoids.

Regarding to complexes **3** and **4**, they are both derived from imine ligands (**HL3** and **HL4**), as confirmed by the N2-C8 distances of 1.282 (7) Å (complex **3**) and 1.245(14) Å (complex **4**), which are typical of C = N bond distances. In both cases, the nitrogen imine atoms are coordinate *trans* to each other and the atoms of the same nature (phenol oxygen and pyridine nitrogen) are mutually *cis*. In complex **3**, the perchlorate atoms Cl and O1 lies in a 2-fold rotation axis, causing a rotational disorder of this anion. Considering the bond distances around the Co(III) center, the equatorial plane consists of two symmetry related nitrogen [Co1-N1: 1.983(4) Å] and oxygen atoms [Co1-O1: 1.867(3) Å]. The axial positions are occupied by the nitrogen atoms from imine [Co1-N2: 1.941(4) Å], as observed for complexes **1** and **2**, where the ligands are coordinate in a meridional form.

For the sake of comparison one can define the equatorial plane of complex **4** by two nitrogen atoms [Co-N1: 1.973(8) Å, Co-N4: 1.942 (10) Å] and by two oxygen atoms [Co-O1: 1.882(7) Å, Co-O4: 1.886 (7) Å]. The axial positions are occupied by two nitrogen atoms from the imine ligand [Co-N2: 1.971(9) Å, Co-N5:1.953(7) Å]. Finally, the coordination sphere of the cobalt atoms in both complexes **3** and **4** are quite similar (Fig. S3).

3.3. Spectroscopies

All complexes were investigated in solution (DMSO-d_6) by NMR spectroscopy and peak attributions are presented in the experimental section. Complex **2** presented very low solubility in DMSO-d_6 and only de ^{1}H NMR was feasible. The spectrum shows mostly double signals which suggest that two structures are present in solution (in a proportion of c.a. 7:3). It might be related to a dynamic equilibrium between geometric isomers that are being recorded in the time scale of the NMR spectroscopy. Conversely, the presence of just one set of peaks in the ^{1}H NMR spectra of complexes **3** and **4** suggests that the mononuclear structures observed in the X-ray analysis are being maintained in solution (Fig. S1).

The electronic spectra of complexes **2**–**4** (Fig. S4) were measured in methanolic solution in the range 200–900 nm in order to compare with a similar measurement performed for complex **1** [26] and the results are presented in Table 3. An accurate comparison is jeopardized

Table 1
Crystallographic data for compounds **2**, **3** and **4**. Data for compound **4** belongs to a heavily twinned sample that loses solvent during the data collection.

Compound	Complex **2**	Complex **3**	$CoBepiNO_2$(Complex **4**)
Chemical formula	$CoC_{28}H_{28}N_6O_6\cdot ClO_4$	$CoC_{28}H_{26}N_4O_2\cdot ClO_4\cdot 2H_2O$	$CoC_{28}H_{24}N_6O_8.ClO_4.2(CH_3COCH_3)$
M_r	702.94	644.94	815.07
Cell setting, space group	Triclinic, *P*-1	Tetragonal, Tetragonal, $P\text{-}42_1c$	Triclinic, *P*1
Temperature (K)	293 (2)	293 (2)	130 (2)
a, *b*, *c* (Å)	10.010 (2), 10.894 (2), 13.670 (3)	11.5145 (16), 11.5145 (16), 21.320 (4)	11.5647(11), 11.7742(8), 13.4975(18)
α, β, γ (°)	90.06 (3), 100.27 (3), 91.61 (3)	90, 90, 90	91.503(9), 99.773(10), 90.928(7)
V (Å^3)	1466.3 (5)	2826.6 (8)	1810.2(3)
Z	2	4	2
Radiation type	Mo *K*α	Mo *K*α	Mo *K*α
μ (mm^{-1})	0.75	0.76	0.63
Crystal size (mm^3)	0.17×0.14×0.04	0.3×0.28×0.13	0.69×0.37×0.25
T_{min}, T_{max}	0.87, 0.97	0.78, 0.948	0.517, 0.7031
R_{int}	0.056	0.038	0.082
$R[F^2>2\sigma(F^2)]$, $wR(F^2)$, *S*	0.049, 0.125, 0.96	0.048, 0.152, 1.12	0.1496, 0.185, 4.4
No. of reflections	5170	2487	4473
No. of parameters	418	205	481
$\Delta\rho_{max}$, $\Delta\rho_{min}$ (e Å^{-3})	0.73, −0.47	0.92, −0.46	1.41, -1.52
Flack parameter		−0.04 (4)	

by the presence of intense charge transfer transition bands bellow 400 nm, which arise from the presence of the imine and $-NO_2$ chromophores.

3.4. Cyclic voltammetry

As the reduction potential of complex **1** was very negative, and far from the ideal range to be accessed by intracellular reductases, the use of electron withdrawing groups in the ligand backbone was expected to anodically shift (to more positive values) this potential. Then, the use of ligands **HL1 – HL4** to synthesize Co(III) complexes was rationalized in order to obtain complexes with the same set of donor atoms in the first coordination sphere of the metal center, but with distinct reduction potentials, since imine and $-NO_2$ electron withdrawing groups were systematically employed. As observed in Fig. 5, in addition to the geometric configuration differences discussed above, the substitution of an amine for an imine anodically shifts the reduction potential of the Co(III) → Co(II) process in 0.74 V for the –H substituent (**1**: $E_{pc} = -1.13$ V *vs* NHE and **3**: $E_{pc} = -0.39$ V *vs* NHE), and in 0.89 V for the $-NO_2$ substituent (**2**: $E_{pc} = -0.89$ V *vs* NHE and **4**: $E_{pc} = 0.00$ V *vs* NHE). The $-NO_2$ group promotes a shift of +0.24 V in the amine-containing complexes (**1** and **2**) and of +0.39 V in the imine ones (**3** and **4**). Comparing the data for complexes **1** and **4**, in addition to the anodic shift, it is also evident the increase of the system reversibility (Fig. 5). In fact, the following reversibility tendency is observed: complex **1** ($\Delta E_p = 2.27$ V)< complex **2** ($\Delta E_p = 1.01$ V)<complex **3** ($\Delta E_p = 0.49$ V)<complex **4** ($\Delta E_p = 0.12$ V). The major effect is observed for complex **4** that combines both groups, imine and $-NO_2$, and presents a positive and reversible process at +55 mV *vs* NHE. According to the crystallographic X-ray data for this complex, a plane is formed by the imine, the phenol and the $-NO_2$ groups, which enables a great electron delocalization over all of them, and probably correlates to the positive and reversible redox potential.

Table 2
Selected bond lengths [Å] and angles [°] for complexes **2**, **3** and **4**.

Complex 2				Complex 3		Complex 4	
Molecule A		Molecule B					
Co1A—O1A	1.885(3)	Co1B—O1B	1.887(2)	Co1—O1	1.867(3)	Co—O1	1.882(7)
Co1A—N2A	1.981(3)	Co1B—N2B	1.982(3)	Co1—N2	1.941(4)	Co—O4	1.886(7)
Co1A—N1A	1.995(4)	Co1B—N1B	1.989(3)	Co1—N1	1.983(4)	Co—N4	1.942(10)
						Co—N5	1.953(7)
						Co—N2	1.971(9)
						Co—N1	1.973(8)
C8A—N2A	1.487(5)	C8B—N2B	1.483(5)	C8—N2	1.282(7)	C8—N2	1.245(14)
O1A—Co1A—N1A	87.73(13)	O1B—Co1B—N1B	87.12(12)	O1—Co1—N1	175.77(16)	O1—Co—O4	90.1(3)
O1A—Co1A—N2A	93.90(12)	O1B—Co1B—N2B	93.46(12)	O1—Co1—N2	93.34(16)	O1—Co—N4	89.1(4)
N2A—Co1A—N1A	88.90(14)	N2B—Co1B—N1B	90.28(13)	N2—Co1—N1	90.48(17)	O4—Co—N4	178.0(4)
$O1A^{ii}$—Co1A—N1A	92.27(13)	$O1B^{i}$—Co1B—N1B	92.88(12)	$O1^{iii}$—Co1—N1	88.23(14)	O1—Co—N5	84.6(3)
O1A—Co1A—$N2A^{ii}$	86.10(12)	O1B—Co1B—$N2B^{i}$	86.54(12)	O1—Co1—$N2^{iii}$	84.63(16)	O4—Co—N5	91.7(3)
N2A—Co1A—$N1A^{ii}$	91.10(14)	N2B—Co1B—$N1B^{i}$	89.72(13)	N2—Co1—$N1^{iii}$	91.50(16)	N4—Co—N5	90.1(4)
O1A—Co1A—$N1A^{ii}$	92.26(13)	O1B—Co1B—$N1B^{i}$	92.88(12)	$O1^{iii}$—Co1—$N1^{iii}$	175.77(16)	O1—Co—N2	90.4(3)
$O1A^{ii}$—Co1A—O1A	180	$O1B^{i}$—Co1B—O1B	180	$O1^{iii}$—Co1—O1	90.3(2)	O4—Co—N2	85.2(3)
$N2A^{ii}$—Co1A—N2A	180	$N2B^{i}$—Co1B—N2B	180	$N2^{iii}$—Co1—N2	177.1(2)	N4—Co—N2	92.9(4)
N1A—Co1A—$N1A^{ii}$	180	$N1B^{i}$—Co1B—N1B	180	$N1^{iii}$—Co1—N1	93.5(2)	N5—Co—N2	174.1(4)
						O1—Co—N1	174.4(4)
						O4-Co-N1	84.3(3)
						N4-Co-N1	96.5(4)
						N5-Co-N1	94.6(3)
						N5-Co-N1	94.6(3)
						N2-Co-N1	90.1(4)

Symmetry codes: (i) $-x\pm1,-y,-z$; (ii) $-x\pm1,-y\pm1,-z\pm1$; (iii) $-x\pm1,-y\pm1,z$.

Table 3
UV–vis ($C = 1.0 \times 10^{-3}$ M) and redox potentials of complexes **2** – **4** in methanol.

Complex	λ_{max}, nm (ε M^{-1} cm^{-1})	E (V *vs* NHE) at 100 mV s^{-1}	
		E_{pc}	E_{pa}
2	595 (680), 375 (3590), 305(3415)	−0.89	+0.12
3	650 (sh), 490 (sh), 390 (17060)	−0.39	+0.10
4	435 (sh), 308 (16450)	0.00	+0.12

sh = shoulder.

3.5. Biological activity

To explore the biological properties of complexes **1** – **4** and to assess the cytotoxicity against tumor cell line, it was measured the effect of complexes and their ligands (**HL1 – HL4**) on viability of *B16F10* cells.

In general, it was observed little effect on cellular viability decrease for all free ligands, where the most pronounced was achieved with **HL1** in concentration higher than 60 μM. For example, in 125 μM their cellular viabilities range from 70 to 100%. However, the coordination to Co(III) enhances their activities and, in 125 μM, cell viability data for complexes **1** – **4** ranges around 22% to 52%, in the following range: **1**>**4**≈**2**>**3** (Table 4). In this concentration, complex **1** showed a decrease of about 45% in cell viability when compared to the same concentration of its free ligand, **HL1**. The major effects are observed for complexes **2** and **3**, where the cell viabilities decrease approximately 65% and 25%, respectively, compared to the free ligands (**HL2** and **HL3**).

The analysis of the cytotoxic properties of (**HL1 – HL4**) suggests that the observed cell-killing effects can be attributed to the coordination of the ligands to Co(III), although the active species responsible for antitumour activity have not been identified and the mechanism related to DNA damage and/or structural modification of DNA or other cellular targets are poorly understood. Apparently, there is no direct correlation between cytotoxicity and the reduction potentials of complexes **1 – 4.** The observed *in vitro* citotoxicity may be related to some oxidative cell damage as well as to structural aspects of the cobalt species.

4. Conclusions

The data presented here show that no straight correlation can be addressed among the substituted backbone ligands, the complexes reduction potentials and their activities. Even though it was possible to modulate the Co(III) → Co(II) reduction potential with the insertion of electron withdrawing groups in the backbone ligands, and achieve values in an accessible range for intracellular reductases, it did not lead to greater cytotoxicity. In addition, as previously observed for **HL1** and complex **1** [26], ligands themselves cannot be considered good effectors since they do not show large effect on cellular viability decrease. This is consistent with the hypothesis that under the conditions assessed, the cytotoxicity occurs due to their complexation to Co(III) but not acting as ligand carriers. Although the mechanism of action was not elucidated, the effect may be due to a cross link between complexes and DNA or proteins, which is a known mechanism of action of different metallodrugs [40–44].

Table 4
Cellular viability and IC_{50} values of cobalt complexes and their ligands on *B16F10* melanoma tumor cell line.

	% cellular viability at 125 μM	IC_{50}
HL1	68.6 ± 16.0	>125 μM
Complex **1**	21.9 ± 5.3	≈60 μM
HL2	101.7 ± 17.9	>125 μM
Complex **2**	35.9 ± 4.49	>60μM and<125 μM
HL3	77.6 ± 17.1	>125 μM
Complex **3**	52.2 ± 0.23	≈125 μM
HL4	90.5 ± 27.0	>125 μM
Complex **4**	30.9 ± 9.0	>60 μM and<125 μM

Abbreviations

HL1	[(2-hydroxybenzyl)(2-(pyridil-2-yl)ethyl]amine)
HL2	[(2-hydroxy-5-nitrobenzyl)(2-(pyridil-2-yl)ethyl]amine);
HL3	[(2-hydroxybenzyl)(2-(pyridil-2-yl)ethyl]imine)
HL4	[(2-hydroxy-5-nitrobenzyl)(2-(pyridil-2-yl)ethyl]imine)
COSY	correlation spectroscopy
HSQC	Heteronuclear single-quantum correlation spectroscopy
HMBC	Heteronuclear multiple-bond correlation spectroscopy
DEPT	Distortionless enhancement by polarization transfer
MTT	3-(4,5-Dimethylthiazol-2-yl)-2,5-diphenyltetrazolium bromide
NHE	Normal Hydrogen Electrode

Acknowledgments

Authors are grateful for the facilities of the LDRX Laboratory (Laboratório de Difração de Raios X da UFF), LabCri (Laboratório de Cristalografia da UFMG), and grants from Capes, CNPq, FAPERJ, FAPEMIG and FAPESP Financial Agencies.

Appendix A. Supplementary material

Crystallographic data for the structures reported have been deposited at the Cambridge Crystallographic Data Center. This information may be obtained free of charge from the Director, CCDC, 12 Union Road, Cambridge, CB2 1EZ, UK (fax: +44-1223-336033; e-mail: deposit@ccdc.cam.ac.uk or http://www.ccdc.cam.ac.uk CCDC numbers 830927, 830928 and 830929). Supplementary materials related to this article can be found online at doi:10.1016/j.jinorgbio.2011.09.011.

References

[1] J.A. Bertout, S.A. Patel, M.C. Simon, Nature Reviews Cancer 8 (2008) 967–975.
[2] J.M. Brown, W.R. Wilson, Nature Reviews Cancer 4 (2004) 437–447.
[3] R.G. Bristow, R.P. Hill, Nature 8 (2008) 180–192.
[4] S.H. van Rijt, P.J. Sadler, Drug Discovery Today 14 (2009) 1089–1097 (and references therein).
[5] C.-H. Zhou, Y.-Y. Zhang, C.-Y. Yan, K. Wan, Lin-Ling Gan, Y. Shi, Anti-Cancer Agents in Medicinal Chemistry 10 (2010) 371–395.
[6] A.V. Klein, T.W. Hambley, Chemical Reviews 109 (2009) 4911–4920.
[7] T.W. Failes, T.W. Hambley, Dalton Transactions (2006) 1895–1901.
[8] T.W. Failes, C. Cullinane, C.I. Diakos, N. Yamamoto, J.G. Lyons, T.W. Hambley, Chemistry A European Journal 13 (2007) 2974–2982.
[9] T.W. Failes, T.W. Hambley, Journal of Inorganic Biochemistry 101 (2007) 396–403.
[10] G.R. Hoffman, G.S. Gessner, J.F. Hughes, M.V. Ronan, K.E. Sylvia, C.J. Willett, Mutation Research 623 (2007) 41–52.
[11] M. Aouida, O. Tounekti, O. Belhadj, L.M. Mir, Antimicrobial Agents and Chemotherapy 47 (2003) 2012–2014.
[12] T.W. Hambley, Science 318 (2007) 17–18.
[13] E. Reisner, V.B. Arion, B.K. Keppler, A.J.L. Pombeiro, Inorganica Chimica Acta 361 (2008) 1569–1583.
[14] T.W. Hambley, Dalton Transactions 43 (2007) 4929–4937.
[15] T.W. Hambley, Science 318 (2007) 1392–1393.
[16] I.Y.A. Levitin, A. Sigan, L. Bubnovskaya, I. Ganusevich, L. Campanella, P. Wardmand, Russian Chemical Bulletin 52 (2003) 2636–2645.
[17] S.P. Osinsky, I. Levitin, L. Bubnovskaya, A. Sigan, I. Ganusevich, A. Kovelskaya, N. Valkovskaya, L. Campanella, P. Wardmand, Experimental Oncology 26 (2004) 140–144.
[18] A. G-One, D.C. Ware, W.A. Denny, W.R. Wilson, Radiation Research 162 (2004) 315–325.
[19] L.L. Parker, S.M. Lacy, L.J. Farrugia, C. Evans, D.J. Robins, C.C. O'Hare, J.A. Hartley, M. Jaffar, I.J. Stratford, Journal of Medicinal Chemistry 47 (2004) 5683–5689.
[20] P.R. Craig, P.J. Brothers, G.R. Clark, W.R. Wilson, W.A. Denny, D.C. Ware, Dalton Transactions 4 (2004) 611–618.
[21] D.C. Ware, P.J. Brothers, G.R. Clark, W.A. Denny, B.D. Palmer, W.R. Wilson, J, Chem. Soc, Dalton Trans, 2000 925–932.

[22] A.G. One, K.J. Botting, A.V. Patterson, D.C. Ware, M. Tercel, W.R. Wilson, Journal of Biochemical Pharmacology 71 (2006) 1683–1694.
[23] M. Vieites, P. Noblia, M.H. Torre, H. Cerecetto, M.L. Lavaggi, A.J. Costa-Filho, A. Azqueta, A. Lopez, A. Monge, B. Parajon-Costa, M. Gonzalez, D. Gambino, Journal of Inorganic Biochemistry 100 (2006) 1358–1367.
[24] M.D. Hall, T.W. Failes, N. Yamamoto, T.W. Hambley, Dalton Transactions 36 (2007) 3983–3990.
[25] D. Gambino, Current Medicinal Chemistry 17 (2010) 3616–3631.
[26] E.T. Souza, L.C. Castro, F.A.V. Castro, L.C. Visentin, C.B. Pinheiro, M.D. Pereira, S.P. Machado, M. Scarpellini, Journal of Inorganic Biochemistry 103 (2009) 1355–1365.
[27] T. Yajima, Y. Shimazaki, N. Ishigami, A. Odani, O. Yamauchi, Inorganica Chimica Acta 337 (2002) 193–202.
[28] R. Viswanathan, M. Palaniandavar, T. Balasubramanian, P.T. Muthiah, J, Chem. Soc, Dalton Trans, 1996 2519–2525.
[29] R. Gagne, C. Koval, G. Licenski, Inorganic Chemistry 19 (1980) 2854–2855.
[30] W.J. Geary, Coordination Chemistry Reviews 7 (1971) 81–122.
[31] T. Mosmann, Journal of Immunological Methods 65 (1983) 55–63.
[32] Nonius, COLLECT, Nonius BV, Delft, The Netherlands, 1998.
[33] A.J.M. Duisenberg, Journal of Applied Crystallography 25 (1992) 92.
[34] G.M. Sheldrick, SADABS; Program for Empirical Absorption Correction of Area Detector Data, University of Göttingen, Germany, 1996.
[35] CrysAlis PRO, Oxford Diffraction Ltd., Version 1.171.33.49a (release 05-10-2009 CrysAlis171 .NET) (compiled Oct 5 2009,17:28:39).
[36] Absorption correction: multi-scan CrysAlis PRO, Oxford Diffraction Ltd., Version 1.171.33.49a (release 05–10–2009 CrysAlis171.NET) (compiled Oct 5 2009,17: 28:39). Empirical absorption correction using spherical harmonics, implemented in SCALE3 ABSPACK scaling algorithm.
[37] G.M. Sheldrick, Acta Crystallographica A64 (2008) 112–122.
[38] C.K. Johnson, in: F.R. Ahm (Ed.), Crystallographic Computing, Munksgaard, Copenhagen, 1970, pp. 207–219.
[39] K. Nakamoto, Infrared and Raman Spectra of Inorganic and Coordination Compounds, 3rd ed John Wiley & Sons, New York, 1977 part II, pp. 231, 232, 242.
[40] E. Gao, X. Gao, F. Guan, M. Zhu, L. Liu, M. Zhang, Y. Zhang, Y. Wang, Z. Wen, Y. Zhang, Y. Zhang, Q. Liang, European Journal of Medicinal Chemistry 46 (2011) 160–167.
[41] T.A. Heinrich, G.V. Poelhsitz, R.I. Reis, E.E. Castellano, A. Neves, M. Lanznaster, S.P. Machado, A.A. Batista, C.M. Costa-Neto, European Journal of Medicinal Chemistry 46 (2011) 3616–3622.
[42] P. Tamil-Selvi, H. Stoeckli-Evans, M. Palaniandavar, Journal of Inorganic Biochemistry 99 (2005) 2110–2118.
[43] S. Srinivasan, J. Annaraj, P. Athappan, Journal of Inorganic Biochemistry 99 (2005) 876–882.
[44] V.A. Kawade, A.A. Kumbhar, A.S. Kumbhar, C. Näther, A. Erxleben, U.B. Sonawane, R.R. Joshi, Dalton Transactions 40 (2011) 639–650.